Journal of Engineering Research and Reports

23(4): 1-14, 2022; Article no.JERR.90654
ISSN: 2582-2926

New Equations for Energy Dissipation down a Stepped Spillway

Okechukwu Ozueigbo [a*] and J. C. Agunwamba [a]

[a] Department of Civil Engineering, Faculty of Engineering, University of Nigeria, Nsukka, Nigeria.

Authors' contributions

This work was carried out in collaboration between both authors. Author OO designed the study, performed the statistical analysis, wrote the protocol and wrote the first draft of the manuscript. Author JCA managed the literature searches. Both authors read and approved the final manuscript.

Article Information

DOI: 10.9734/JERR/2022/v23i417602

Open Peer Review History:
This journal follows the Advanced Open Peer Review policy. Identity of the Reviewers, Editor(s) and additional Reviewers, peer review comments, different versions of the manuscript, comments of the editors, etc are available here: https://www.sdiarticle5.com/review-history/90654

Original Research Article

Received 11 June 2022
Accepted 14 August 2022
Published 31 August 2022

ABSTRACT

Stepped spillways use their stepping nature to substantially dissipate energy in floodwater. Many researchers investigated the hydraulic and geometric relationships of the stepped spillway with a dam slope above 26.6^o degrees that resulted in energy dissipation. But few studied stepped spillways with a dam slope below 26.6^o degrees that also resulted in energy dissipation with even fewer proposing models that estimated its energy losses. This resulted in limited information and guidelines for designers of stepped spillways involved with slopes below 26.6^o degrees. The authors reviewed researchers' publications on horizontal stepped spillways with dam slopes between $3.4^o \leq \theta \leq 26.6^o$ conducted in transition and skimming flows in large-size facilities with phase-detection intrusive probes. They obtained data sets from them, which they reanalyzed to develop 2 new energy dissipation models that govern skimming flows over a wide range of operating conditions. The data from the new models compared well with the measured data in terms of energy dissipation with high coefficients of correlation between 0.95 and 0.99. All data were in good agreement independent of channel slopes, stepped configuration, and sensor size. The models are simple, easy to use, and render more accurate results than the existing model.

Keywords: Aerated flow; energy dissipation; chute slope; dam height; stepped spillway; skimming flow.

**Corresponding author: Email: Ozueigbo.okechukwu.pg78995@unn.edu.ng, okechukwuozueigbo@gmail.com;*

ABBREVIATIONS

d_c : Critical water depth (m)
Fr : Froude number = $F_r = \frac{q_w}{\sqrt{gd^3}}$
H_1 : Residual head at the bottom of the spillway (m)
ΔH : Difference between the maximum head and the residual head (m)
H : Total head (m)
H_{max} : Maximum head available (m)
H_{max} : $H_{dam} + 3/2 * d_c$
Q : Discharge ($m^2 s^{-1}$)
q_w : Discharge per unit width ($m s^{-1}$)
Reynolds number defined as: $Re = \rho_w * U_w * D_H / \mu_w$
U_w : Flow velocity (m/s): $U_w = q_w/d$
W : Channel width (m)

SUBSCRIPTS

c – Conditions at Critical Height
N– Number of Step

1. INTRODUCTION

Major damage may occur if the energy of floodwater, especially its kinetic energy, is not dissipated safely. One type of flood release facility is the stepped spillway. Their steps offer significant resistance to flow that result in energy dissipation. This loss in energy leads to the design of smaller and more economical dissipation structures downstream of the chute. As the discharge down the chute is increased, the critical discharge would be reached, beyond which air would be entrained in the flow. This phenomenon is known as a two-phase flow or Air-Water flow.

Researchers like [1-7] in the last decades, experimentally investigated air-water flows on stepped spillways with a dam slope above 26.6O degrees. They provided vast information and guidelines for its design.

But few studied stepped spillways with a dam slope below 26.6o degrees, which resulted in energy dissipation with fewer proposing models that estimate its energy losses. This resulted in limited information and guidelines for designers of stepped spillways with slopes below 26.6o degrees. There is also a dearth of design rules and publications for stepped spillways; hence, the need for additional study on stepped spillways. Thus, the authors conducted a study that resulted in better equations and provided design engineers with the knowledge of the impact of a stepped spillway on energy dissipation performance.

Essery ITS [8] identified three kinds of flows that occur over a stepped spillway. Such flows include:

a) nappe flow regime, b) transition flow regime, and c) skimming flow regime.

In the nappe flow regime, a sequence of water flows down from one step to the next lower step with the formation of a hydraulic jump at each step. This type of flow can be likened to a sequence of separate drop structures linked together [9,10].

Nappe flow with an established hydraulic jump (Fig. 1) usually occurs from small discharges with shallow flow depths. It flows from one step to the next step below it with the formation of supercritical at the edges of the steps and returns to subcritical flow downstream of the jump at each fall. A hydraulic jump is formed at each drop; energy losses accompany it [3,11].
The losses occur due to

a) The disintegration of the spout in the air [8,12],
b) The blending of flow on the steps, with or without the development of hydraulic jump on the step [11].

Energy losses could be computed using equations [1.1] or [1.2].

$$\frac{\Delta H}{H_o} = 1 - \frac{\frac{d_1}{d_c} + \frac{1}{2}\left(\frac{d_c}{d_1}\right)^2}{\frac{3}{2} + \frac{H_{dam}}{d_c}} \quad (1.1)$$

Where d_1 is the water depth at impact, d_c is the critical water depth, and H_{dam} is the dam height, ΔH is the energy loss, H_o is the maximum available energy, h is the height of the spillway step [3] later expressed this equation in terms of the spillway step height, the critical flow depth, and the dam height as:

$$\frac{\Delta H}{H_o} = 1 - \left[\frac{0.54\left(\frac{d_c}{h}\right)^{0.275} + \frac{3.43}{2}\left(\frac{d_c}{h}\right)^{-0.55}}{\frac{3}{2} + \frac{H_{dam}}{d_c}}\right] \quad (1.2)$$

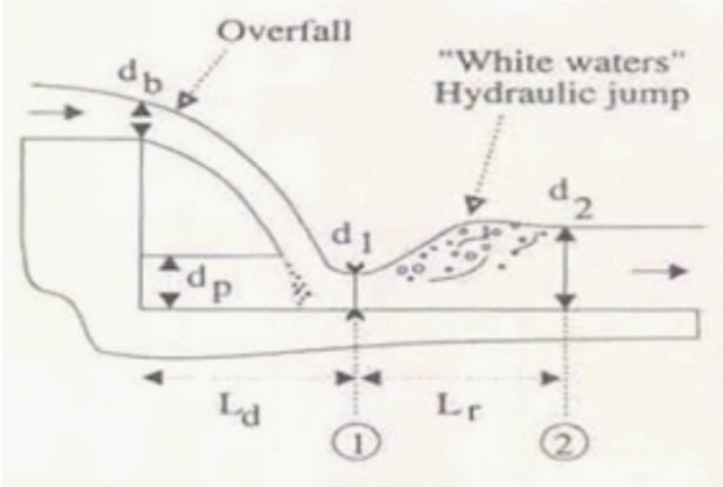

Fig. 1. Nappe flow regime (Flow at a drop structure)

Several researchers like [13] examined the flow regime change from nappe to skimming in a spillway and linked the parameters to flow critical depth, dc, and the spillway shape, which are the non-dimensional ratios dc /h and h/ l.

Rajaratnam N, [11] took into consideration these non-dimensional parameters and proposed that values of dc/h > 0.8 in the range of 0.42< h/l <0.842 will yield skimming flow, exiting the nappe flow regime when flow rate becomes dc/h < 0.8 whatsoever the geometric specifications of the structure might be.

Studies have, however, shown that the majority of the changes in flow regime occur for the flow rate, d_c/h, less than this proposed 0.8.

The skimming flow regime occurs with the submergence of the steps with the development of a fully aerated uniform flow downstream of a long chute. Along the upstream steps, a non-aerated flow region exists in which a turbulent boundary layer develops. Air entrainment in the flow begins where the boundary layer intersects the free surface, referred to as the point of inception. Downstream of the point of inception, the flow continues to aerate and varies gradually in depth (Fig. 2). The flow eventually becomes a fully aerated uniform flow in which the water depth, velocity, and air concentration become constant [14,15] (Fig. 3).

Energy is dissipated to keep stable depression vortices. If uniform flow conditions are reached downstream of the spillway, the energy loss could be calculated as follows [15] (Fig. 4):

$$\frac{\Delta H}{H_{max}} = 1 - \frac{\left(\frac{d_w}{d_c}\right)\cos\theta + \frac{1}{2}\left(\frac{d_c}{d_w}\right)^2}{\frac{H_{dam}}{d_c} + \frac{3}{2}} \quad (1.3)$$

Where d_w is the clear water depth, U_{avg} is the average velocity, the total head loss may be rewritten in terms of the friction factor, f, the spillway slope, θ, in degree, the critical depth, d_c, and the dam height, H_{dam}:

$$\frac{\Delta H}{H_{max}} = 1 - \frac{\left(\frac{f}{8sin\theta}\right)^{1/3} cos\theta + \frac{E}{2}\left(\frac{f}{8sin\theta}\right)^{-2/3}}{\frac{H_{dam}}{d_c} + \frac{3}{2}} \quad (1.4)$$

Eq [1.4] was computed for spillway slope with θ = 52 (degrees) and friction factor, f = 0.3 and f = 1.30, that represent average flow resistance on smooth spillways and stepped spillways, respectively. where E is the kinetic energy correction coefficient, θ is the dam slope in degrees.

[5,4,16], Felder S and [17], and [18] have published works on the impact, of scale effects in modeling stepped spillways.

The scale effect is defined as slight misrepresentations, which occur when secondary forces like viscous forces and surface tension forces in turbulent flow are ignored. They are usually overlooked in many open-channel flows. However, if they are ignored in highly air-entrained flows in stepped spillways, where they play significant roles, they could lead to scale effects and wrong interpretations of results [19-22].

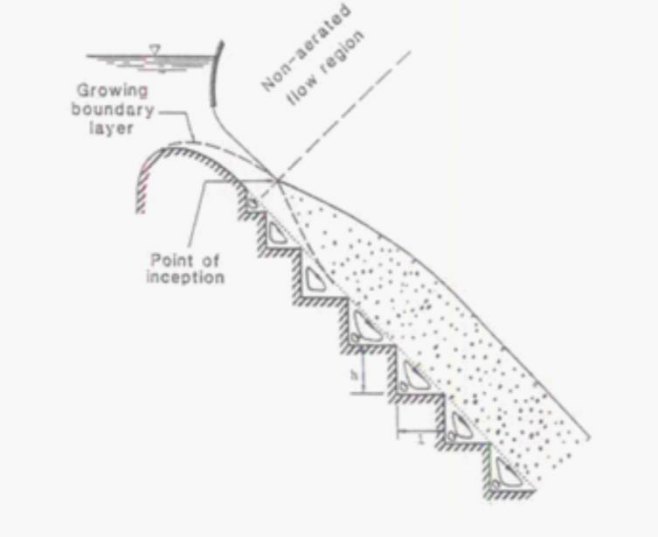

Fig. 2. Skimming flow regime - Sorensen (1985)

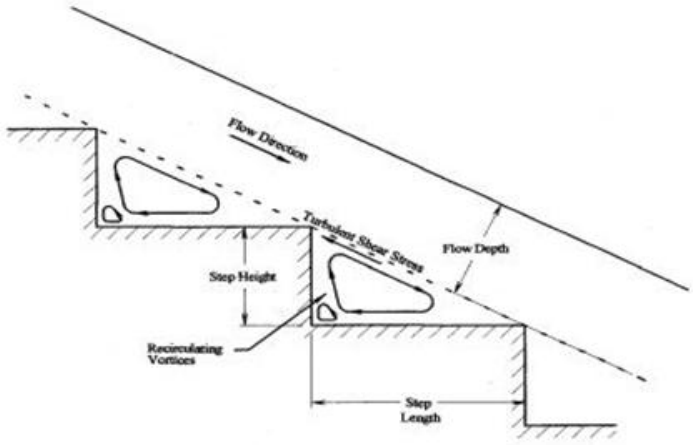

Fig. 3. Skimming flow regime with uniform flow conditions

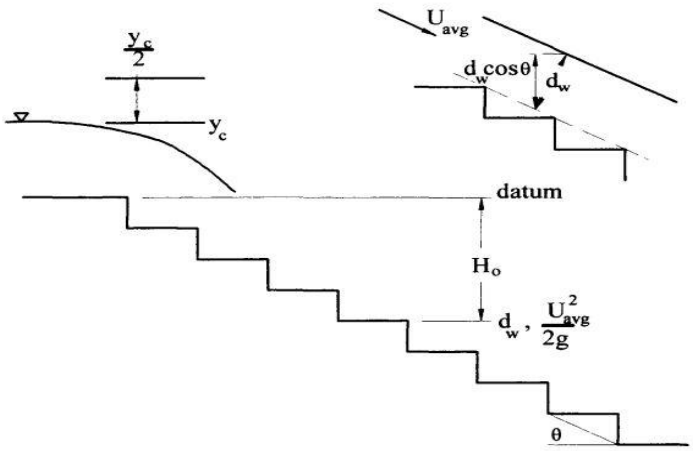

Fig. 4. Arrangement of the spillway with the definition of the variables

Scale effects in stepped spillway models are likely to occur with scales lower than 10:1, Reynolds number smaller than 1 x 10^5, Weber number smaller than 100, and step heights lesser than 3 cm.

2. MATERIALS AND METHODS

The authors carefully selected from the literature 11 No publications (listed in Table 1) on horizontal stepped spillways with minimum step heights of 3 cm, undistorted Froude values, and large dimensionless discharges corresponding to Reynolds numbers between 1×105 and 1×10^6.

The researchers used experimental facilities on large scale to minimize scale effects that affect the air-water flow processes in high-velocity free-surface flows [17]. They measured air-water flow properties at all step edges downstream of the inception point of air-entrainment with conductivity phase-detection intrusive probes and optical fiber probes.

Use of a Dall Tube flow meter, or V-notch for flow rates, Prandtl-Pitot for flow velocities, or Point gauge for clear water flow depth to obtain air-water flows properties is not practicable as large quantities of air are entrained at the air-water interface [23,24].

The principle of the conductivity probe is based on the difference between the resistivity of air and water, which provides an instantaneous voltage signal [25,26]. The threshold technique analyzes signals - from a single sensor - used to calculate a) the time-averaged local air concentration or void fraction C, b) the number of air-to-water (or water-to-air) voltage changes expressed as bubble count rate F, and c) the air bubble and water droplet chord sizes. For a double-tip conductivity probe with longitudinal separation between the two probe sensors, the cross-correlation analysis of the signals leads to the local time-averaged interfacial velocity V [15].

Details about signal processing techniques can be found in [10] and [27].

The double-tip conductivity probes used had sensor sizes of Ø = 0.13 mm and 0.25 mm and were sampled for a period of 45 s with a frequency of 20 kHz per sensor.

The discharges comprised transition and skimming flow rates 0.035 ≤ q_w ≤ 0.234 m2/s for the spillways with θ = 8.9° and 0.02 ≤ q_w ≤ 0.249 m2/s for θ = 26.6◦ comprising Reynolds numbers of 1.4 × 10^5 ≤ Re ≤ 9.3 × 10^5 and 8.1 × 10^4 ≤ Re ≤ 9.9 × 10^5 (Table 1).

Table 1 lists the selected publications, the channel slope, the step height h, the channel width W, the flow rate per unit width q_w, the flow rate d^c/h with dc the critical flow depth.

2.1 Formulation of the Models

The authors obtained more than 700 data sets from the 11 No researchers (Table 1). They reanalyzed about 500 with complete data to formulate energy dissipation models that govern transition and skimming flow over a wide range of operating conditions.

In modeling, it is necessary to determine the values of the parameters that can fit the model of the system it shall describe [28]. By the least square method, the best fit curve for this study was as:

$$\frac{\Delta H}{H_{max}} = \left[\alpha_o \frac{Nh}{y_c}\right]^{\alpha_1} N^{\alpha_2} h^{\alpha_2} \theta^{\alpha_3} \quad (2.1)$$

Where

$\frac{\Delta H}{H_{max}}$ is the energy loss ratio,
H_{max} is the maximum available height,
N is the number of spillway steps,
h is the height of the spillway steps,
θ is the spillway channel slope.

They used a portion of the measured data sets and multiple regression analysis to solve Equation [2.1] which yielded the values of the constant α_o along with the coefficients α_1, α_2, α_3, and α_4, which are then substituted in Equation [2.1] to give the developed models in 3.1.

They used the remaining portion to evaluate the model's performance.

Table 1. Summary of the 11 No Publications for the flat stepped spillway with chute angle of 3.4° ≤ θ ≤ 26.6°

References	Slope (θ)deg	Step geometry and Flow conditions	Instrumentation	N (No of Step)
[29]	21.8	h (cm) = 10 dc/h = 1.0 –1.57 qw (m^2/s)= 0.095-0.18 Re =$3.8x10^5 - 7.2x10^5$	Double-tip (Ø=0.25mm) 20kHz/45s	10
[30]	21.8	h (cm) = 5 dc/h = 1.17 – 3.16 qw (m^2/s)= 0.059 - 0.10 Re =$2.4x10^5 - 4.0x10^5$	Double-tip (Ø=0.25mm) 20kHz/45s	20
[31]	26.6	h (cm) = 10 dc/h = 0.5 - 1.7 qw (m^2/s)= 0.03 - 0.217 Re =$1.2x10^5 - 8.7x10^5$	Double-tip (Ø=0.025mm) 20kHz/45s	10
[32]	3.4	h (cm) = 14.3 dc/h = 0.61 - 0.92 qw (m^2/s) = 0.08 - 0.15 Re =$3.2x10^5 - 6.0x10^5$	N/A	10
[33]	18.4 & 26.6	h (cm) = 3 & 6 dc/h = 2.65 - 3.58 qw (m^2/s)= 0.07 - 0.11 Re =$2.8x10^5 - 4.4x10^5$	N/A	2.4 m H_{dam}
[34]	3.4	h (cm) = 7.15 & 11.3 dc/h = 0.61 - 1.85 qw (m^2/s) = 0.08 - 0.15 Re =$3.2x10^5 - 6.0x10^5$	Single-tip (Ø=0.35mm) 5kHz/60s & 180s	10 & 18
[35]	5.7 & 11.3	h (cm) = 0.63 & 5.0 dc/h = 1.25 - 14.3 qw (m^2/s)= 0.02 - 0.08 Re =$0.8x10^5 - 3.2x10^5$	Single-tip (Ø=0.1mm) 2kHz/60s	
[36]	14.6	h (cm) = 5 & 10 dc/h =1.27 - 3.55 qw (m^2/s)= 0.05 - 0.234 Re =$2.0x10^5 - 9.4x10^5$	Double-tip (Ø=0.13mm) 30kHz/40s	26

References	Slope (θ)deg	Step geometry and Flow conditions	Instrumentation	N (No of Step)
[34]	15.9 & 21.8	h (cm) = 10 dc/h = 0.78 - 1.53 qw (m^2/s)=0.069 – 0.188 Re =$2.8x10^5 - 7.5x10^5$	Double-tip (Ø=0.025mm) 20kHz/20s	9
[37]	15.9	h (cm) = 5 & 10 dc/h = 0.6 - 3.2 qw (m^2/s)= 0.021 - 0.22 Re =$5.0x10^5 - 8.8x10^5$	Double-tip (Ø=0.025mm) 20kHz/20s	9 & 18
[38]	18.4 & 26.6	h (cm) = 3 & 6 dc/h = 2.65 – 3.58 qw (m^2/s)= 0.07 - 0.11 Re =$2.8x10^5 - 4.4x10^5$	Double-tip (Ø=0.13mm) 25kHz/25s	2.4 m H_{dam}
[37]	21.8	h (cm) = 10 dc/h = 1.1 –1.7 qw (m^2/s)= 0.114 - 0.22 Re =$4.6x10^5 - 8.8x10^5$	Double-tip (Ø=0.025mm) 20kHz/20s	10
[18]	8.9	h (cm) = 5 dc/h = 1.0 – 3.55 qw (m^2/s)=0.035 – 0.234 Re =$1.4x10^5 - 9.4x10^5$	Double-tip (Ø=0.13mm) 20kHz/45s	21
[18]	26.6	h (cm) = 5 & 10 dc/h = 0.69 – 3.30 qw (m^2/s)= 0.02 – 0.227 Re =$0.8x10^5 - 9.1x10^5$	Double-tip (Ø=0.25mm) 20kHz/45s	10 & 20
[18]	26.6	h (cm) = 10 dc/h = 0.82 – 1.85 qw(m^2/s)= 0.073 – 0.249 Re =$2.9x10^5 - 1.0x10^6$	Double-tip (Ø=0.25mm) 20kHz/45s	20

3. RESULTS AND DISCUSSION

3.1 Developed Models for Skimming Flow Regimes

3.1.1 Eq [3.1] is valid for use when h (cm) is not more than 20, N is not more 20, θ (degrees) is between 26.6° and 21.8°, and d_c/h is between 1.0 and 3.7.

$$\frac{\Delta H}{H_{max}} = \left[0.049\frac{Nh}{d_c}\right]^{0.353} N^{0.06}h^{0.124}\theta^{-0.157} \quad (3.1)$$

3.1.2 Eq [3.2] is valid for use when h (cm) is not more than 20, N is not more 20, θ (degrees) is between 21.8° and 3.4°, and d_c/h is between 1.0 and 3.6.

$$\frac{\Delta H}{H_{max}} = \left[0.029\frac{Nh}{d_c}\right]^{0.353} N^{0.06}h^{0.124}\theta^{-0.157} \quad (3.2)$$

3.2 Charts for 3.1.1

Figs. 5 to 8 depicted the energy loss rates as a function of the expression of a dam height divided by the critical depth for the measured data, the developed analytical formulation (Eq. [3.1]), the existing model for the computation of energy dissipation (Eq. [1.4]) with the friction factors of f = 0.30 and 1.30. The figures also show some traditional concave shape distributions for all the plotted four data sets for energy dissipation for all the flow rates. As seen in the charts, energy losses increase with decreasing discharges and increase with increasing spillway height following earlier investigations [6,35,3]. The measured data and the developed model data (Eq. [3.1]) are in close agreement with the coefficients of correlation from 0.96 to 0.99. Again, measured data are in close agreement with the existing model data (Eq. [1.4]) with a friction factor, f = 0.3, yielding the coefficients of correlation between 0.92 and 0.95

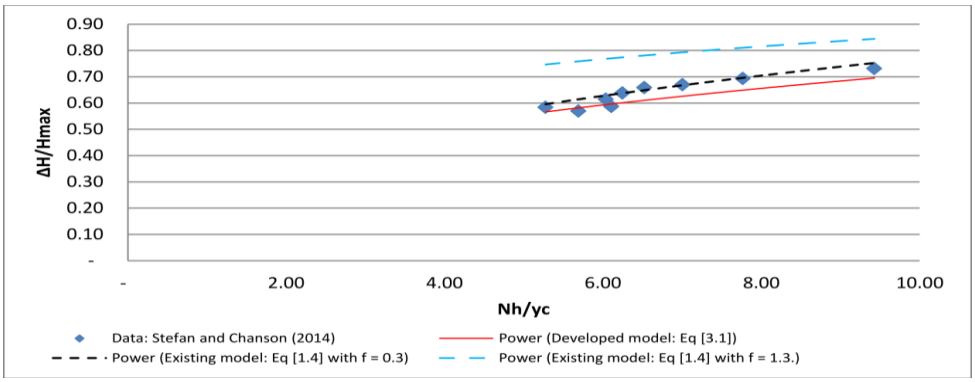

Fig. 5. $\Delta H/H_{max}$ as a function of Nh/d_c for θ = 26.6, N = 10, h= 10, q_w = (0.073 - 0.249) m^2 s^{-1} & Re = (2.92×10^5 - 9.96×10^5), flow rate d_c/h of (0.82 - 1.85).

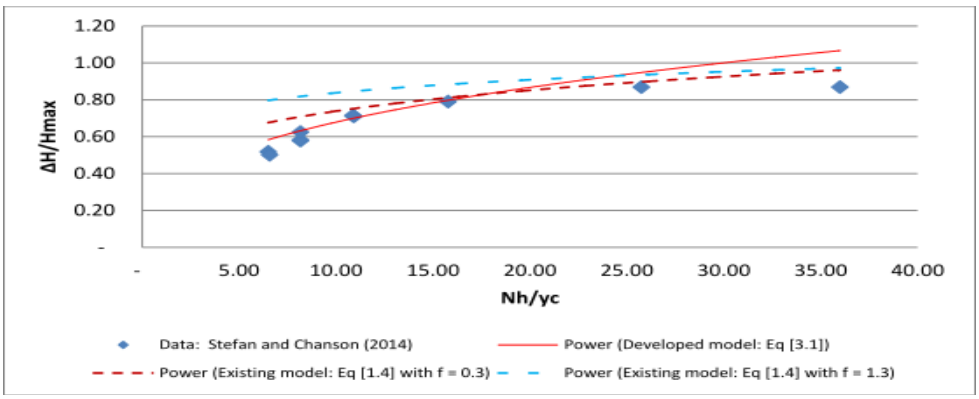

Fig. 6. $\Delta H/H_{max}$ as a function of Nh/d_c for θ = 26.6, N = 20, h = 5, q_w = (0.020 - 0.227) m^2 s^{-1} & Re = (8.0×10^4 - 9.08×10^5), flow rate d_c/h, of (0.69 - 3.30).]

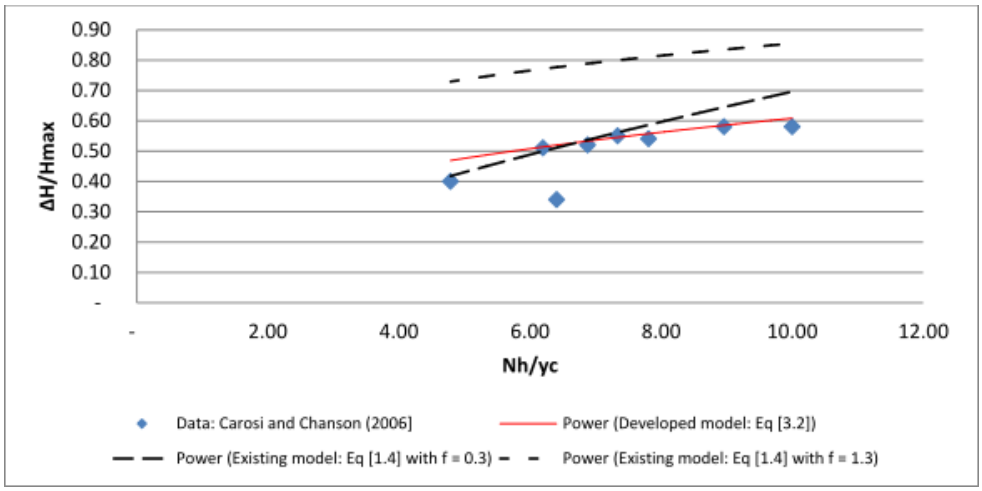

Fig. 7. $\Delta H/H_{max}$ as a function of Nh/d_c for θ = 21.8, N = 10, h = 10, q_w = (0.095 - 0.180) $m^2 s^{-1}$, Re = (3.80×10^5 - 7.20×10^5), flow rate, dc/h, of (1.00 - 1.57)

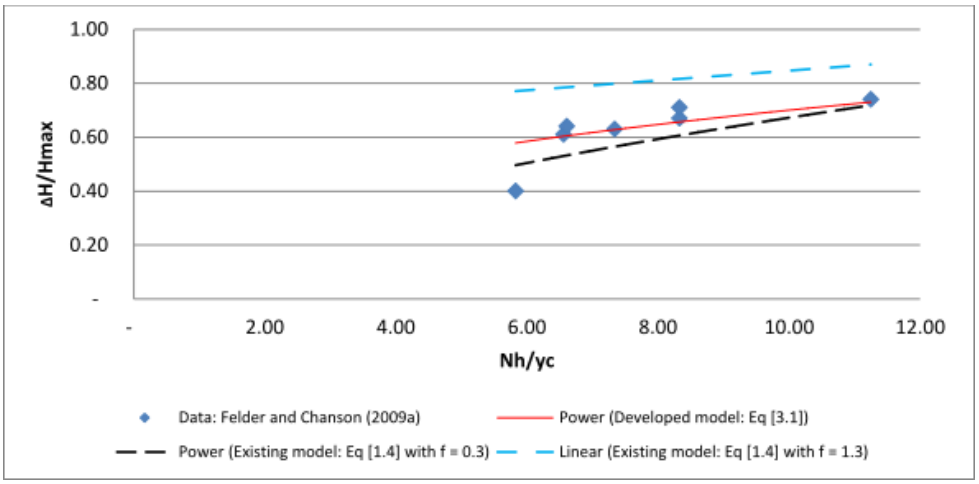

Fig. 8. $\Delta H/H_{max}$ as a function of Nh/d_c for θ = 21.8, N = 20, h = 5, q_w = (0.059 - 0.158) $m^2 s^{-1}$, Re = (2.36×10^5 - 6.32×10^5), flow rate, d_c/h, of (0.80 - 1.85)

3.3 Charts for 3.1.2

Figs. 9 to 14 depicted the energy loss rates as a function of the expression of a dam height divided by the critical depth for the measured data, the developed analytical formulation (Eq. [3.2]), the existing model for the computation of energy dissipation (Eq. [1.4]) with f = 0.10, 0.30, and 1.3. They displayed similar traditional concave shape distributions for all plotted four data sets for energy dissipation for all flow rates. As shown in the charts, energy losses increase with decreasing discharges and increase with rising dam heights that follow earlier investigations [6,34,3]. They showed that measured data sets, the developed model data (Eq. [3.2]), and the existing model data (Eq. [1.4]) with friction factor, f = 0.3, are in close agreement with the coefficients of correlation from 0.95 to 0.99. Fig. 9 showed that the developed model data (Eq [3.2]) was slightly higher than the measured data, increasing with increasing discharges. Fig. 10 indicated that the developed model compared well with the measured data than the existing model with f = 0.10. Figs. 11, 12, and 13 showed that the developed model compared well with the measured data sets. Fig. 14 shows that the developed model predicted values slightly lower than the measured data, while the existing model with f = 0.10 produced data sets higher than the measured data sets.

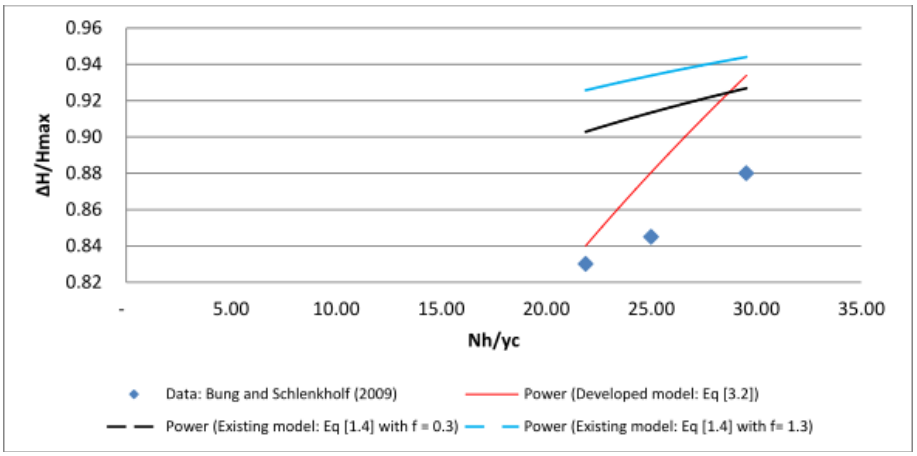

Fig. 9. $\Delta H/H_{max}$ as a function of Nh/d_c for θ = 18.4, N=40, h = 6, q_w = (0.059 - 0.158m) $m^2 s^{-1}$, Re = (2.36×10^5 - 6.32×10^5), flow rate, d_c/h, of (0.80 - 1.85)

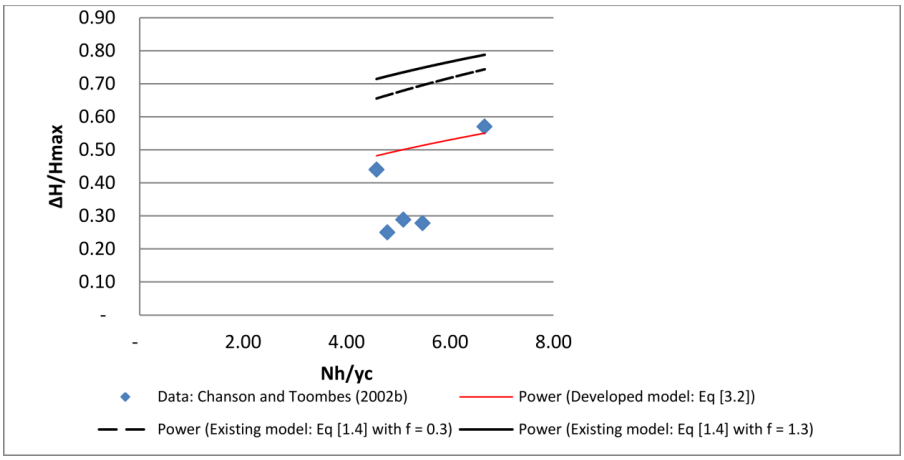

Fig. 10. $\Delta H/H_{max}$ as a function of Nh/d_c for θ =15.9, N = 9, h = 10, q_w = (0.069 - 0.188) $m^2 s^{-1}$, Re = (2.76×10^5 - 7.52×10^5), flow rate, dc/h, of (0.78 - 1.53)

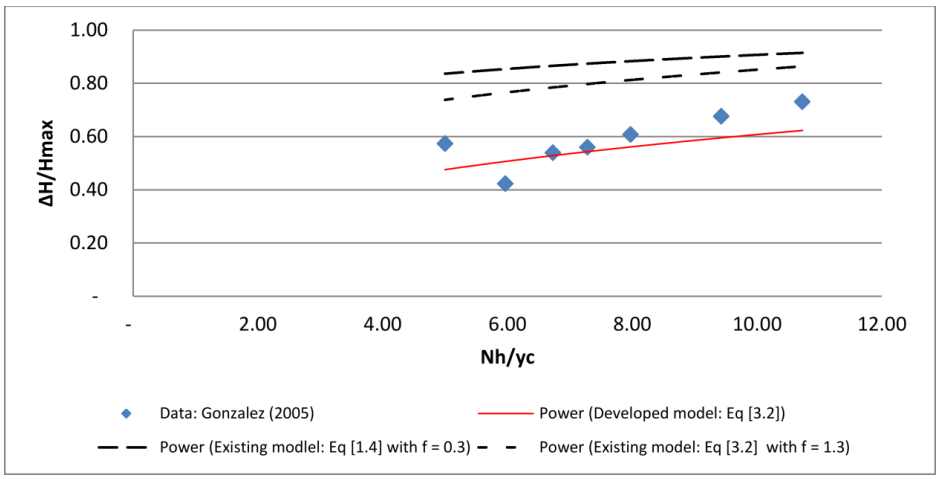

Fig. 11. $\Delta H/H_{max}$ as a function of Nh/d_c for θ = 15.9, N = 18, h = 5, q_w = (0.021 - 0.220) $m^2 s^{-1}$, Re = (8.4×10^3 - 8.8×10^5), & flow rate, dc/h of (0.60 - 3.20)

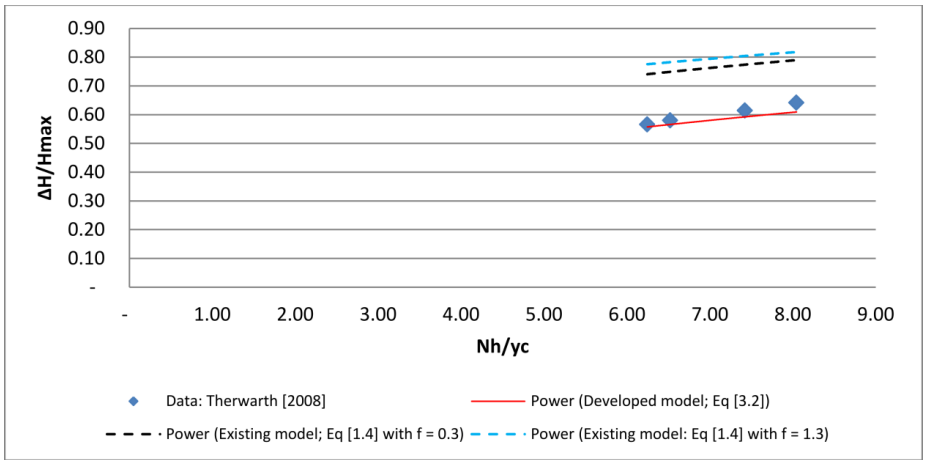

Fig. 12. $\Delta H/H_{max}$ as a function of Nh/d_c for θ = 14.6, N = 13, h = 10, q_w = (0.05 - 0.234) $m^2 s^{-1}$, Re = (2.0 x 10^5 - 9.36 x 10^5), & flow rate, dc/h, of (1.27 - 3.55)

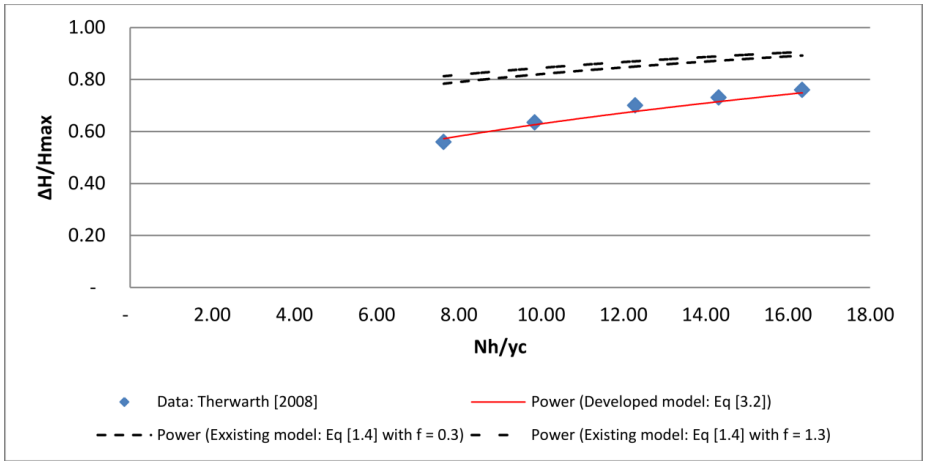

Fig. 13. $\Delta H/H_{max}$ as a function of Nh/d_c for θ = 14.6, N = 26, h = 10.0, q_w = (0.05 - 0.234) $m^2 s^{-1}$, Re = (2.0 x 10^5 - 9.36 x 10^5), & flow rate, d_c/h, of (1.27 - 3.55)

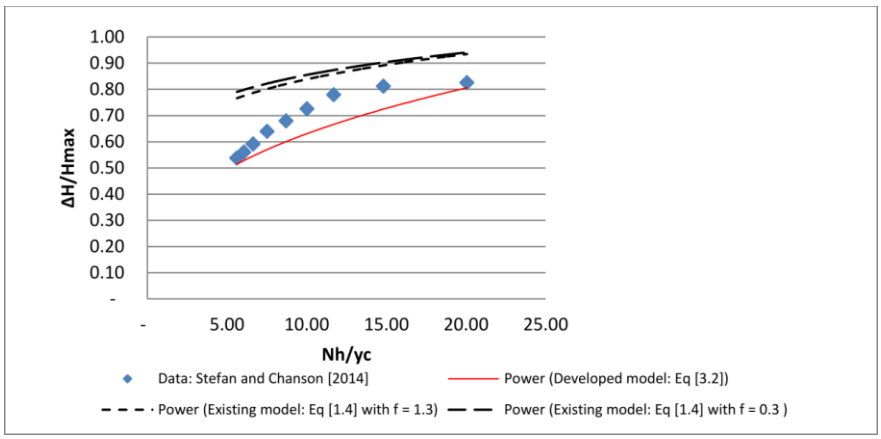

Fig. 14. $\Delta H/H_{max}$ as a function of Nh/d_c for θ = 8.9, N = 21, h = 3, q_w = (0.035 - 0.234) $m^2 s^{-1}$, Re = (1.40 x 10^5 - 9.36 x 10^5), & flow rate, dc/h, of (1.0 - 3.55)

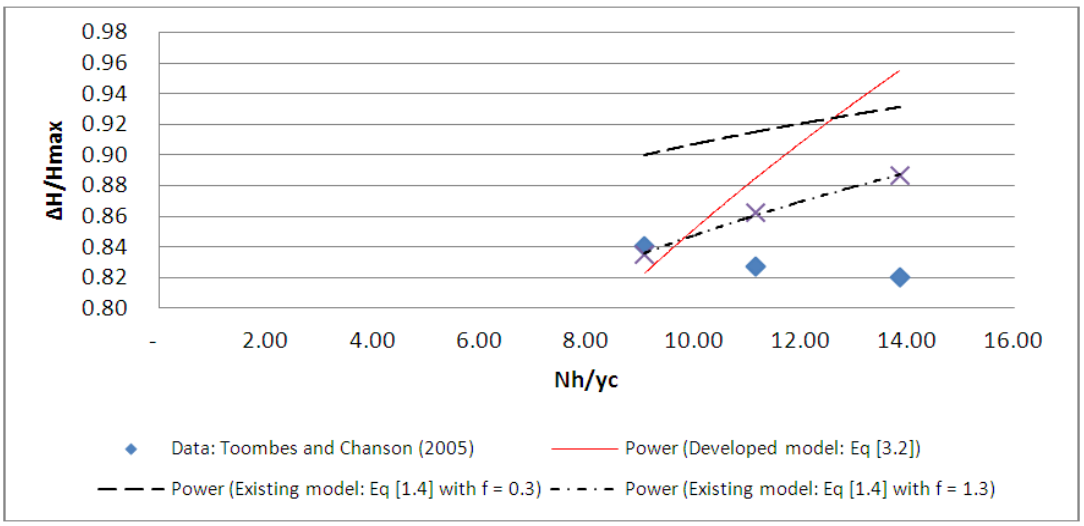

Fig. 15. $\Delta H/H_{max}$ as a function of Nh/dc for q_w = (0.61 - 0.92m^2/s), Re = (2.44 x 10^6 - 3.68 x 10^6), & flow rate, dc/h, of 0.82 - 1.85

Fig. 15 showed an interesting pattern: Rates of energy losses with a stepped spillway slope of 3.4^o degrees reduced along the spillway with decreasing discharges and decreased with increasing stepped spillway height.

So, there is a need to investigate further why this incidence occurred in future.

4. CONCLUSION

Two new models for rates of energy losses in horizontal stepped spillways with slopes below 26.6o degrees, with data based on detailed phase-detection probe measurements were developed. Their generated data compared well with the measured data sets. The new models also produced data sets that were in close agreement with the existing equation for rates of energy losses with friction factor, f = 0.10. Rates of energy losses increased along the stepped spillway with decreasing discharges and increased with increasing stepped spillway heights. However, rates of energy losses with a stepped spillway slope of 3.4o degrees decreased along the spillway with decreasing discharges and decreased with increasing stepped spillway height.

ACKNOWLEDGEMENTS

We acknowledge the fruitful discussions with Prof Hubert Chanson of the Department of Civil Engineering, The University of Queensland, Brisbane QLD 4072, Australia.

COMPETING INTERESTS

Authors have declared that no competing interests exist.

REFERENCES

1. Horner MW. An analysis of flow on cascades of steps, PhD thesis, Univ. of Birmingham, U.K; 1969.
2. Peyras L, Royet P, Degoutte G. Flow and Energy Dissipation over Stepped Gabion Weirs." Jl of Hyd. Engrg. ASCE. 1992;118(5):707-717.
3. Chanson H. Air bubble entrainment in open channels. Flow structure and bubble size distributions. Int J Multiph Flow. 1997a; 23(1):193–203
4. Chanson H. Measuring air–water interface area in supercritical open channel flow. Water Res. 1997b;31(6):1414–1420
5. Boes RM. Scale effects in modeling two-phase stepped spillway flow. In Proc. Intl. Workshop on Hydraulics of Stepped Spillways, Minor HE and Hager WH, eds. Steenwijk, The Netherlands: A. A. Balkema. 2000:53-60.
6. Matos J, Frizell KH, André S, Frizell KW. On performance of velocity measurement techniques in air-water flows. In Proc. Hydraulic Measurements and Experimental Methods 2002, CD-ROM. T. L. Wahl, C. A. Pugh, K. A. Oberg, and T. B. Vermeyen, eds. Reston, Va.: ASCE; 2002.
7. Thorwarth J. Hydraulisches Verhalten der Treppengerinne mit eingetieften Stufen -

Selbstinduzierte Abflussinstationaritäten und Energiedissipation. PhD Thesis, University of Aachen, Germany (in German); 2008.

8. Essery ITS, Horner MW. The hydraulic design of stepped spillways, Rep. 33, Construction Industry Research and Information Assoc., London, U.K; 1971.
9. Chamani MR, Rajaratnam N. Jet Flow on Stepped Spillways. J. Hydraul. Engg. ASCE 1994;120(2):254–259.
10. Chanson H. Air–water flow measurements with intrusive phase-detection probes. Can we improve their interpretation? J Hydraul Eng ASCE. 2002;128(3): 252–255,
11. Rajaratnam N. Skimming flow in stepped spillways. J. Hydr. Engrg., ASCE. 1990;116(4):587-591.
12. Moore WL. Energy Loss at the Base of a Free Overfall. Trans. ASCE. 1943;108: 1343–1360
13. Beitz E, Lawless M. Hydraulic Model Study for darn on GHFL 3791 lsaac River al Burton Gorge. Water Resources Commission Report, Ref. No. REP/24.1, Sept., Brisbane, Australia; 1992.
14. Bindo M, Gautier J, Lacrotx F. The Stepped Spillway of :Vl"Bah Darn. lntl Water Power and Dam Construction. 1993;1-5(1):35-36.
15. Chanson H. The hydraulics of stepped chutes and spillways. Balkema, Lisse. 2001:418
16. Boes RM, Hager WH. Two-phase flow characteristics of stepped spillways. J. Hydraul. Eng. ASCE. 2003a;129(9): 661-670.
17. Felder S, Chanson H. Turbulence, dynamic similarity and scale effects in high-velocity freesurface flows above a stepped chute. Exp Fluids. 2009b;47(1): 1–18
18. Stefan Felder, Hubert Chanson. Aeration and air–water mass transfer on stepped chutes with embankment dam slopes, Environ Fluid Mech; 2014.
    DOI 10.1007/s10652-014-9376-x
19. Felder S, Chanson H. Energy dissipation and flow resistance on flat slope stepped spillways. 5th IAHR International Symposium on Hydraulic Structures, Brisbane, Australia, 25-27 June 2014. Brisbane, Australia: The University of Queensland; 2014.
    Available:https://doi.org/10.14264/uql.2014.22
20. Felder S, Chanson H. Air–water flow properties in step cavity down a stepped chute. Int J Multiph Flow. 2011;37(7): 732–745
21. Meireles I, Matos J. Skimming flow in the nonaerated region of stepped spillways over embankment dams. J Hydraul Eng ASCE. 2009;135(8):685–689 .
22. Toombes L, Chanson H (2005) Air–water mass transfer on a stepped waterway. J Environ Eng ASCE 131(10):1377–1386.
23. Chanson H, Carosi G. Advanced post-processing and correlation analyses in high-velocity air– water flows. Environ Fluid Mech. 2007;7(6):495–508.
24. Chanson H, Toombes L. Air–water flows down stepped chutes: turbulence and flow structure observations. Int J Multiph Flow. 2002a;28(11):1737–1761.
25. Chanson H, Toombes L. Supercritical Flow at an Abrupt Drop: Flow Patterns and Aeration". Can. J. Civil Eng. 1998;25(5):956–966.
26. Degouite G, Peyras L, Royet P. Skimming Flow in Stepped Spillways - Discussion. Jl of Hyd. Engrg., ASCE. 1992;118(1): 111-114.
27. Felder S. Air–water flow properties on stepped spillways for embankment dams: aeration, energy dissipation and turbulence on uniform, non-uniform and pooled stepped chutes. PhD Thesis, The University of Queensland, Australia; 2013.
28. Agunwamba JC. Engineering Mathematical Analysis. 2007;479-510; 674-675.
    (ISSN 978-8137-08-3).
29. Carosi G, Chanson H.Air-water time and length scales in skimming flow on a stepped spillway. Application to the spray characterisation. Report No. CH59/06, Division of Civil Engineering, The University of Queensland, Brisbane, Australia, July; 2006.
30. Felder S, Chanson H. Energy dissipation, flow resistance and gas-liquid interfacial area in skimming flows on moderate-slope stepped spillways. Environ Fluid Mech. 2009a;9(4):427–441.
31. Guenther P, Felder S, Chanson H. Flow aeration, cavity processes and energy dissipation on flat and pooled stepped spillways for embankments. Environ Fluid Mech. 2013;13(5):503–525.

32. Toombes L. Experimental study of air–water flow properties on low-gradient stepped cascades. PhD Thesis, Dept. of Civil Engineering, University of Queensland, Australia; 2002.
33. Bung DB, Schlenkhoff A. Prediction of oxygen transfer in self-aerated skimming flow on embankment stepped spillways, 33rd IAHR World Congress. Vancouver, Canada 123 Author's personal copy Environ Fluid Mech; 2009.
34. Chanson H, Toombes L. Energy dissipation and air entrainment in stepped storm waterway: experimental study. J Irrig Drain Eng ASCE. 2002b;128(5): 305–315.
35. Ohtsu I, Yasuda Y, Takahashi M (2004) Flow characteristics of skimming flows in stepped channels. J Hydraulic Eng ASCE 130(9):860–869. DOI:10.1061/~ASCE0733-9429~2004!130:9~860
36. Takahashi M, Yasuda Y, Ohtsu I.. Effect of Reynolds number on characteristics of skimming flows in stepped channels. In Proc. 31st Biennial IAHR Congress, 2880-2889. B. H. Jun, S. I. Lee, I. W. Seo, and G. W. Choi, eds. International Association for Hydro-Environment Engineering and Research; 2005.
37. Gonzalez CA. An experimental study of free-surface aeration on embankment stepped chutes. PhD Thesis, Department of Civil Engineering, The University of Queensland, Brisbane, Australia; 2005.
38. Bung DB. Zur selbstbelüfteten Gerinneströmung auf Kaskaden mit gemäßigter Neigung. PhD Thesis, Lehr- und Forschungsgebiet Wasserwirtschaft und Wasserbau, Bergische Universitaet Wuppertal, Germany (in German);2009.

Peer-review history:
The peer review history for this paper can be accessed here:
https://www.sdiarticle5.com/review-history/90654